# Voltage-Sensing Residues in the S2 and S4 Segments of the *Shaker* K⁺ Channel

Sang-Ah Seoh, Daniel Sigg, Diane M. Papazian, and Francisco Bezanilla
Departments of Physiology and Anesthesiology
School of Medicine
University of California, Los Angeles
Los Angeles, California 90095-1751

## Summary

The activation of *Shaker* K⁺ channels is steeply voltage dependent. To determine whether conserved charged amino acids in putative transmembrane segments S2, S3, and S4 contribute to the gating charge of the channel, the total gating charge movement per channel was measured in channels containing neutralization mutations. Of eight residues tested, four contributed significantly to the gating charge: E293, an acidic residue in S2, and R365, R368, and R371, three basic residues in the S4 segment. The results indicate that these residues are a major component of the voltage sensor. Furthermore, the S4 segment is not solely responsible for gating charge movement in *Shaker* K⁺ channels.

## Introduction

The open probability of voltage-dependent ion channels is regulated by the membrane potential. To achieve this regulation, charged or dipolar voltage sensors in the channel protein respond to changes in the membrane potential and initiate conformational changes that lead to channel opening (Hodgkin and Huxley, 1952). The rearrangement of charged components in the voltage sensor produces nonlinear displacement currents called gating currents that can be recorded experimentally (Armstrong and Bezanilla, 1973). As originally shown by Hodgkin and Huxley, the voltage dependence of many Na⁺ and K⁺ channels is quite steep: the equivalent of at least four to six electronic charges ($e_0$) must move across the entire transmembrane electric field for a channel to open (Hodgkin and Huxley, 1952). In *Shaker* K⁺ channels, the equivalent of 12–13 $e_0$ traverses the electric field upon the activation of a single channel (Schoppa et al., 1992). This represents the total nonlinear gating charge movement per channel, z, in units of $e_0$.

To understand the mechanism of voltage-dependent activation at the molecular level, it is important to identify the parts of the channel protein that contribute to gating charge movement. The prime candidates include charged amino acid side chains that may move in response to changes in the electric field, although structures with intrinsic dipole moments, such as α helices, may also contribute. In voltage-gated Na⁺, Ca²⁺, and K⁺ channels, the fourth putative transmembrane segment (S4) contains conserved, regularly spaced, positively charged residues, making it a candidate for the voltage sensor (Noda et al., 1984; Catterall, 1986; Guy and Seetharamulu, 1986).

Studies combining mutagenesis and functional analysis have provided support for this role of the S4 (Stuhmer et al., 1989; Papazian et al., 1991; Liman et al., 1991; Logothetis et al., 1992; Perozo et al., 1994). More recently, the environment of positions in and near the S4 segment has been probed after replacing residues with cysteine. The voltage-dependent reactivity of such cysteines with sulfhydryl-specific reagents or fluorescent probes has provided evidence that the environments of S4 residues change upon activation (Yang and Horn, 1995; Mannuzzu et al., 1996; Yang et al., 1996; Larsson et al., 1996). These studies have focused on the S4 segment. However, segments S2 and S3 contain conserved, negatively charged residues that may also be involved in sensing voltage (Papazian et al., 1995; Planells-Cases et al., 1995). The contribution of charged residues in the S2, S3, and S4 segments to the gating charge movement per channel, z, has not been determined. In this paper, we present direct evidence that four residues contribute to the charge that constitutes the gating current that flows during channel activation. Although our data indicate that the S4 segment is a major contributor to the charge movement, it does not comprise the whole voltage sensor in *Shaker* channels.

## Results

To determine whether the conserved charged residues in segments S2, S3, and S4 contribute to the voltage sensor, we have measured z, the total valence of the gating charge movement per channel, after neutralizing these charged residues one at a time (Figure 1). We have studied five positively charged and three negatively charged residues: R362, R365, R368, R371, and K374 in S4; E283 and E293 in S2; and D316 in S3. D316 and R368 were replaced by the neutral amino acid asparagine, whereas the other residues were replaced by the neutral amino acid glutamine. For control experiments, some charge-conserving mutations were also made.

Neutralizing the pore residue D447 by substitution with asparagine prevents ionic conduction, making it infeasible to determine the value of z using methods that rely on measuring ionic currents. However, evidence from experiments with the charge-conserving mutant D447E indicates that residue 447 can contribute to a binding site for both tetraethyl ammonium (TEA) and external potassium (S.-A. S. and D. M. P., unpublished data), suggesting that it faces into solution, hence experiencing little of the transmembrane voltage.

Mutations were generated in a construct of the *Shaker* channel (ShB-IR) in which residues 6–46 have been deleted to remove N-type inactivation (Hoshi et al., 1990), allowing us to measure the quasi-steady-state properties of ionic and gating currents (Bezanilla et al., 1991).

The valence of the gating charge movement per channel z was estimated in two ways. In the first method, the number of channels (N) in a patch of Xenopus oocyte membrane was estimated by nonstationary fluctuation analysis of macroscopic ionic currents (Sigworth, 1980),
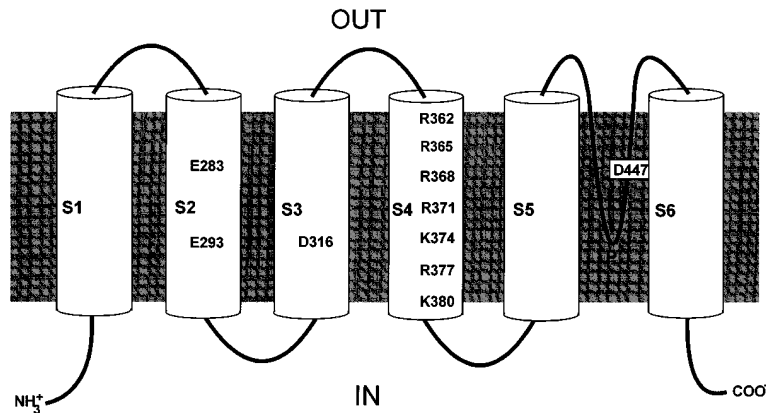
OUT

and then, after blocking the ionic current, the total non-linear charge movement (Q) was determined from the integral of gating current in the same patch. The value of z (called $z_{Q/N}$) was obtained from Q/N and expressed in units of the elementary charge $e_0$. If there is any charge movement that is not required for channel opening, it will also be measured by this method. In the second method, z was estimated by measuring the limiting slope of the conductance at very negative potentials where the probability of channel opening approaches zero (Almers, 1978). This method estimates only the charge movement that leads directly to channel opening, which will be called $z_s$, in units of $e_0$.

## The Voltage Dependence of the Charge Movement and Open Probability

The accurate determination of the total charge (Q) and the number of channels (N) requires that we know the steady-state values of Q and the open probability ($P_o$) versus voltage. To measure the total Q in each mutant, the entire voltage range where the charge moves must be spanned. Likewise, determining N by fluctuation analysis is only accurate when $P_o \geqslant 0.5$; therefore, the range of potentials where $P_o > 0.5$ must be determined.

Using the cut-open oocyte voltage clamp (Stefani et al., 1994), we determined the relative open probability as a function of voltage ($P_o$–V curve) in conducting mutants and the voltage dependence of gating charge movement (Q–V curve) in nonconducting mutants containing the pore-blocking mutation W434F (Perozo et al., 1993).

Figure 2 shows representative curves of the voltage dependence of Q and $P_o$ for the mutants studied. Except for the mutant R362Q, the data have not been normalized to unity. Instead, the maximum value of the charge has been scaled to correspond to $z_{Q/N}$, and the absolute value of $P_o$ for each mutant was estimated by fluctuation analysis of the ionic currents at a given potential. The highest open probabilities achieved ranged from 0.52 to 0.74 in the mutants compared with 0.72 in ShB-IR (Table 1).

Two of the mutants require special comment because their properties affected the determination of $z_{Q/N}$. In R362Q, a mutation that neutralizes the outermost positive charge of the S4 segment, gating charge moves at potentials where a large fraction of the channels have

already opened (Figure 2E). This may indicate the presence of at least two open states with different conductances. In R365Q, the $P_o$–V curve is shifted in the hyperpolarized direction. At −90 mV, a fraction of the R365Q channels are in a long-lived inactivated state. Owing to this persistent inactivation, ionic currents recorded from a holding potential of −150 mV were about 25% larger than those recorded from a holding potential of −90 mV, preceded by a 50 ms prepulse to −120 mV.

## Determination of $z_{Q/N}$ by Measuring Ionic and Gating Currents in the Same Patch

Ionic and gating currents were recorded from an excised, inside-out patch (Hamill et al., 1981). The number of channels, N, was estimated by nonstationary fluctuation analysis of the ionic current (Sigworth, 1980). After blocking the ionic current, the total gating charge movement (Q) was recorded from the same patch. Alternatively, Q was measured in the presence of K$^+$ at the reversal potential with 1 mM K$^+$ on both sides of the membrane (see Experimental Procedures). Representative data for the determination of Q and N are shown in Figure 3. Except for R362Q (data not shown), a parabolic relationship between the variance and the mean current was seen, leading to accurate estimates of N. In R362Q, however, a parabolic relationship was seen for short pulses but not for longer pulses. This result is consistent with the presence of at least two open states with different conductances, as suggested by the Q–V and $P_o$–V curves (Figure 2E). In this mutant, it was not possible to obtain a reliable estimate of N and consequently of $z_{Q/N}$. In R365Q, which is partially slow-inactivated at −90 mV, it was not feasible to maintain patches at a holding potential of −150 mV while acquiring the large number of traces required to estimate N with fluctuation analysis. Therefore, the value of N was corrected by the fraction of channels inactivated at −90 mV, which was the holding potential used during the data collection.

The values of $z_{Q/N}$ for each of the mutants are shown in Figure 4. In ShB-IR channels, $z_{Q/N}$ was about 13 $e_0$, in good agreement with a previous report (Schoppa et al., 1992). Four neutralization mutations, E293Q in S2 ($z_{Q/N}$ = 6–7 $e_0$), R365Q in S4 (8 $e_0$), R368N in S4 (6 $e_0$), and R371Q in S4 (7 $e_0$), reduced $z_{Q/N}$ significantly compared with that of ShB-IR (13 $e_0$). In contrast, E283Q in S2 did not decrease the value of $z_{Q/N}$. Mutant D316N in
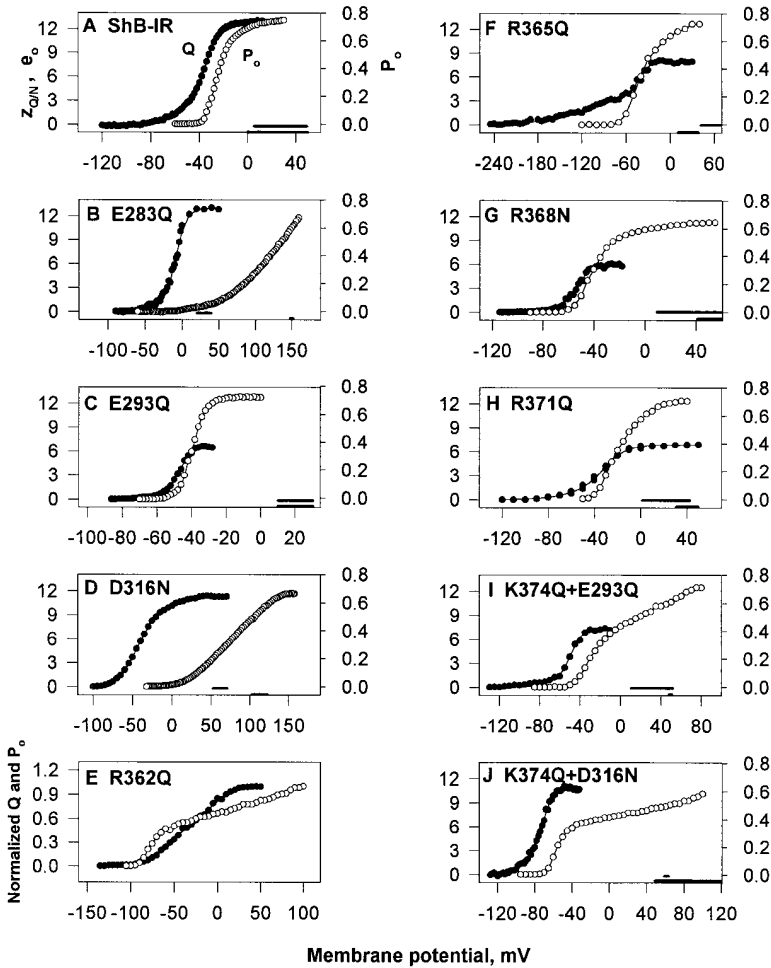
Figure 2. Representative Q–V and $P_o$–V Curves of the Mutants Studied

$P_o$–V relationships (open circles) were obtained from analysis of isochronal tail currents. Except for R362Q (E), all the Q–V relationships (closed circles) have been scaled according to the value of $z_{Q/N}$ (Figure 4), and the $P_o$–V relationships have been scaled according to the $P_o$ values measured by the mean-variance procedure (Table 1). All the Q–V and $P_o$–V curves were obtained with the cut-open oocyte technique, except for R365Q (F), which was obtained with macropatches. $P_o$–V was determined in symmetrical 120 K$^+$ except for K374Q+D316N (J), which was determined in 120 K$^+$ inside and 60 K$^+$ outside, and ShB-IR (A) and R371Q (H), which were determined in 110 K$^+$-glutamate and 2.5 K$^+$ outside. Q–V relationships were obtained using nonconducting mutants in symmetrical 120 K$^+$ for D316N, E293Q, and K374Q+E293Q; symmetrical 0 K$^+$ for ShB-IR, R362Q, R365Q, and R371Q; and internal 120 K$^+$ an external 120 Na$^+$ for E283Q and K374Q+D316N. Upper bars indicate the voltage range used for gating current measurements, and the lower bars indicate the voltage range used to measure the ionic currents for the Q/N experiments.

S3 showed a small decrease in $z_{Q/N}$ (about 2 $e_o$) but, given the errors inherent in the measurement, this decrease is not highly significant (p = 0.07).

It was not possible to determine directly the effect of the S4 mutation K374Q on $z_{Q/N}$, because this mutation eliminates functional expression (Papazian et al., 1991; Perozo et al., 1994), but we were able to analyze its effects in the double mutant combinations E293Q+K374Q and D316N+K374Q, which restore channel activity (Papazian et al., 1995). In E293Q+K374Q, $z_{Q/N}$ was

Table 1. Open Probability and Single Channel Current as Determined from Fluctuation Analysis

| Mutant | i (pA) Mean ± SD | $P_o$ Mean ± SD | Test pulse for i and $P_o$ (mV) | Number of Experiments |
|---|---|---|---|---|
| ShB-IR | 0.83 ± 0.09 | 0.72 ± 0.02 | 30 | 3 |
| E283Q | 1.06 ± 0.21 | 0.55 ± 0.07 | 150 | 2 |
| E293Q | 0.98 ± 0.17 | 0.72 ± 0.07 | 30 | 8 |
|  | 0.04 ± 0.01[a] | 0.63 ± 0.18 | −90[a] | 4 |
| D316N | 1.25 ± 0.23 | 0.58 ± 0.08 | 120 | 3 |
| R365Q | 0.67 ± 0.15 | 0.73 ± 0.01 | 30 | 2 |
| R368N | 0.97 ± 0.21 | 0.64 ± 0.08 | 50 | 6 |
| R371Q | 1.00 ± 0.12 | 0.70 ± 0.07 | 30 | 7 |
|  | 0.05 ± 0.01[a] | 0.52 ± 0.08 | −90[a] | 6 |
| K374Q+E293Q | 0.91 ± 0.19 | 0.61 ± 0.07 | 50 | 9 |
|  | 0.05 ± 0.003[a] | 0.61 ± 0.15 | −90[a] | 3 |
| K374Q+D316N | 1.46 ± 0.27 | 0.64 ± 0.17 | 120 | 3 |
| E293D | 0.05 ± 0.01[a] | 0.74 ± 0.15 | −90[a] | 5 |
| R368K | 0.06 ± 0.002[a] | 0.53 ± 0.05 | −90[a] | 2 |

The table indicates the single-channel current, i, determined by fluctuation analysis; the absolute $P_o$ (= $I_i$/(Ni)); and the test potential used to estimate i.

[a] Experiments using symmetrical 1 mM K$^+$ solutions in which the single-channel current was determined from tail currents at −90 mV.

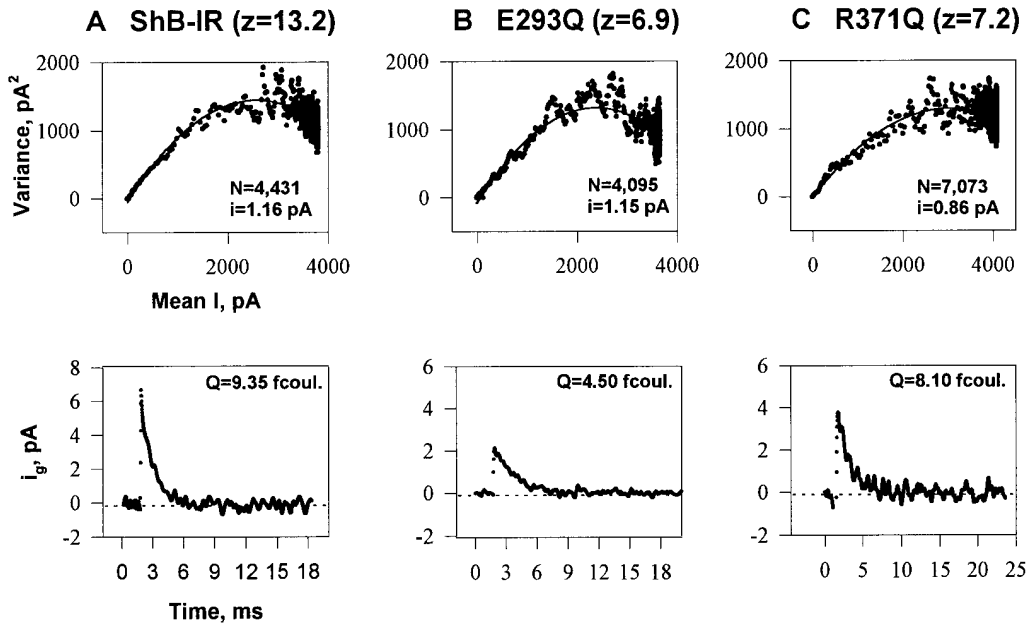## A ShB-IR (z=13.2)  B E293Q (z=6.9)  C R371Q (z=7.2)



Figure 3. Representative Experimental Data for Estimating $z_{Q/N}$

Data obtained from ShB-IR (A), E293Q (B), or R371Q (C). The upper row shows mean current (I) versus variance ($\sigma^2$) plots. From a holding potential of $-90$ mV, the mean ionic current was determined from more than 150 current traces recorded at $+50$ mV for ShB-IR and E293Q and at $+30$ mV for R371Q. Values of N and i are indicated. The bottom row shows gating current measurements. Each panel corresponds to the same patch from which ionic current measurements were made. Ionic currents were blocked by replacing $K^+$ in the internal solution with 110 mM $TEA^+$. Values of the total charge Q obtained by integrating the gating current record are indicated.

about 7.4 $e_0$, whereas it was about 11.1 $e_0$ in D316N+ K374Q. These values are very similar to those of the individual acidic neutralization mutations E293Q and D316N, indicating that K374 does not contribute significantly to the gating charge. In control experiments, we measured $z_{Q/N}$ in the charge-conserving mutant channels E293D and R368K, and as expected, obtained values of about 13 $e_0$ as in ShB-IR.

Our results show that, of the residues studied, only the negatively charged residue at position 293 in S2 and the positively charged residues at positions 365, 368, and 371 in S4 contribute significantly to the gating current.

### Charge Movement Coupled to Channel Opening

To determine the value of z that is energetically coupled to channel opening, $z_s$, we determined the slope of the logarithm of the g–V curve at low open probabilities ($\sim 10^{-3}$). In these experiments, the conductance was not determined from isochronal tail currents, which are small in amplitude at low $P_o$ and therefore significantly contaminated with off-gating currents. Instead, the value of $P_o(V)$ was estimated from the value of g(V) obtained from currents elicited by slow voltage ramps (see Experimental Procedures). The function S(V), which is the slope of ln g (scaled by $kT/e_0$), was plotted as a function of V; at sufficiently low $P_o$, this curve will reach a plateau equal to the actual value of the limiting slope, $z_s$ (Figure 5; Table 2). For E293Q and R368N, a clear plateau was observed providing a good estimate of $z_s$ (Figure 5; Table 2). In several cases, however, the voltage range of our experiments did not reach low enough

values of $P_o$, and no definite plateau was observed, as shown for ShB-IR, D316N, and R365Q in Figure 5. In these cases, the values of the slope represent a lower estimate of $z_s$, indicated in Table 2 with a greater than sign. These lower estimates of $z_s$ were lower than the value of $z_{Q/N}$ for the same mutant. This is not surprising, because charge movement was observed at potentials more negative than the potential used to estimate $z_s$ (compare Figures 2 and 5).

Knowing the Q–V relationship, we can estimate the correct limiting value of $z_s$ by adding the missing charge movement using the following equation

$$\frac{kT}{e_0}\frac{d}{dV}\ln P_o(V) = z - \frac{Q(V)}{N}$$

in which z is the total valence (in units of $e_0$) and Q(V) is the charge moved by all channels (in units of $e_0$) as a function of the membrane potential V. This relation applies to any channel in which gating is subject to the following general assumptions: first, the open state is reached only after all the charge z has moved; second, the contribution of the membrane potential to the free energy of the channel is linear with respect to the gating charge; and third, the distribution of conformations follows the Boltzmann principle. An analytical proof for the general case will be presented elsewhere (D. S. and F. B., unpublished data). We assumed that this relation applies to *Shaker* channels. Defining $Q_{max}$ as the total charge movement, we plotted $(Q_{max} - Q)/Q_{max}$ versus voltage and then we normalized this plot to $z_s$ at the

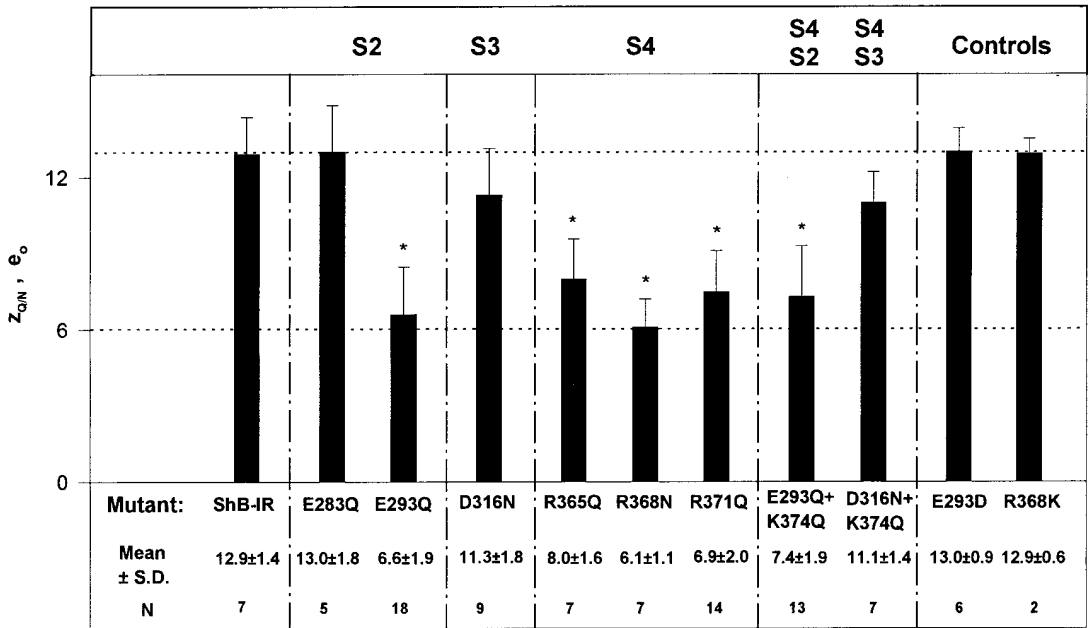| | S2 | | S3 | S4 | | | S4 S2 | S4 S3 | Controls | |
|---|---|---|---|---|---|---|---|---|---|---|
| **Mutant:** | ShB-IR | E283Q | E293Q | D316N | R365Q | R368N | R371Q | E293Q+ K374Q | D316N+ K374Q | E293D | R368K |
| **Mean ± S.D.** | 12.9±1.4 | 13.0±1.8 | 6.6±1.9 | 11.3±1.8 | 8.0±1.6 | 6.1±1.1 | 6.9±2.0 | 7.4±1.9 | 11.1±1.4 | 13.0±0.9 | 12.9±0.6 |
| **N** | 7 | 5 | 18 | 9 | 7 | 7 | 14 | 13 | 7 | 6 | 2 |

Figure 4. A Bar Graph Summarizing $z_{Q/N}$ Values

Below the histogram, under the names of the mutant constructs, are the average $z_{Q/N}$ values ± SD. The number of experiments is indicated in the bottom row. The upper dotted line represents a value of $z_{Q/N} = 13$ $e_0$, while the lower dotted line corresponds to $z_{Q/N} = 6$ $e_0$. Q/N measurements were performed as described in Experimental Procedures. An asterisk indicates those $z_{Q/N}$ values that were significantly different ($p < 0.0001$) than that of ShB-IR, assessed using the unpaired t test. For D316N, $p = 0.073$, and for D316N+K374Q, $p = 0.033$. In all others, $p > 0.81$. To remove resting inactivation of the gating charge movement, hyperpolarizing prepulses, ranging from −120 to −150 mV, were applied from the holding potential of −90 mV, for 50–200 ms before recording gating currents. In R365Q, gating charge movement was detected at very negative potentials, starting at about −240 mV. A prepulse to −150 mV for 200 ms was applied to this mutant; a correction was made to account for gating charge, which moves at potentials more negative than −150 mV based on the Q–V curve. In this mutant, ionic currents were recorded from a holding potential of −90 mV with a prepulse to −120 mV for 50 ms. The values of N were corrected by the slow inactivation removed by a holding potential of −150 mV.

middle of the voltage range, $V_s$, where $z_s$ was measured. To obtain a corrected value $z_c$, we added to $z_s$ all charge moving at potentials more hyperpolarized than $V_s$ (Table 2). The value of $z_s$ for the control channel ShB-IR was 10.9 $e_0$. After correction, a value of 12.6 $e_0$ was obtained for $z_c$. Both of these values agree, within experimental error, with the value of $z_{Q/N}$ (Figure 4). This result is consistent with the view that all the gating charge is coupled to channel opening in ShB-IR channels. Further support for this conclusion is shown by the agreement of S(V) and $z_{Q/N}(Q_{max} − Q)/Q_{max}$ in Figure 5.

The mutations E293Q, R365Q, R368N, R371Q, and K374Q+E293Q that significantly reduce $z_{Q/N}$ also reduce $z_s$. The values of $z_c$ agree, within error, with the values of $z_{Q/N}$ (see Table 2, where $z_c$ and $z_{Q/N}$ are listed in the last two columns). Therefore, the remaining 6–7 $e_0$ are directly coupled to channel opening in these mutant channels.

In the mutant R362Q, the value of $z_s$ cannot be corrected using this procedure because the Q–V and $P_o$–V relations suggest at least two open states with different conductances with charge moving between these states, which is incompatible with one of the above assumptions. The value of 8.7 $e_0$ in R362Q would not include charge moving between the open states. Given this, it is possible that the value of z is normal in this mutant.

## Discussion

The value of the gating charge may be estimated from the steepness of the steady-state activation curve. This open probability ($P_o$) versus voltage (V) curve measures only the z energetically linked with the opening of the channel. Hodgkin and Huxley (1952) used steady-state activation curves in ascribing z the value of 4–6 in the case of Na$^+$ and K$^+$ channels in the squid axon. The main disadvantage of this method is that the interpretation is, in general, model dependent. However, it was first pointed out by Almers (1978) that, assuming only that activation follows a linear sequence of states, the slope of log($P_o$) versus V approaches the total z for very low values of $P_o$ (limiting slope technique). Calculations of $z_s$ in *Shaker* gave values of about 9.5 with $P_o \approx 10^{-2}$ (Schoppa et al., 1992). Another way to measure z is to determine the total charge Q and the number of channels N in the same preparation. In *Shaker* channels, $z_{Q/N}$ has a value of 12–13 $e_0$ (Schoppa et al., 1992). The main disadvantage of this method is that it includes any charge movement, some of which may not be energetically coupled to channel opening. In this study, we have extended the limiting slope measurements to a $P_o$ of $10^{-3}$ to determine $z_s$ and have also estimated $z_{Q/N}$ in channels containing charge-neutralization mutations. Significantly, we have obtained similar values for $z_c$ and
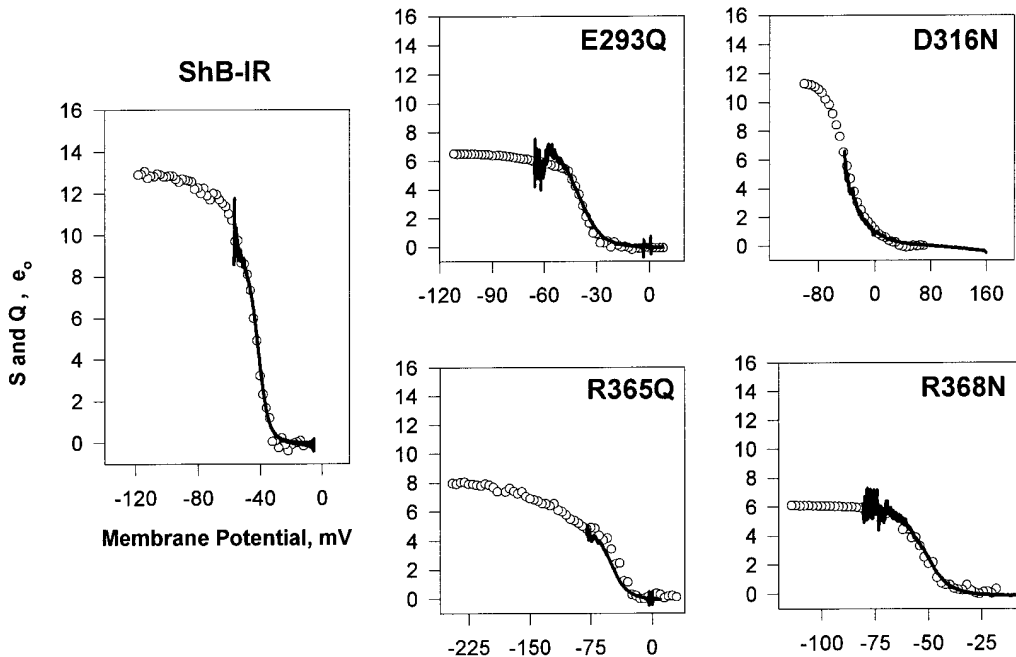
Figure 5. Examples of Superimposed S(V) and $z_{Q/N}(Q_{max} - Q)/Q_{max}$

The continuous lines correspond to the value of $S = (kT/e_0)(d \ln g/dV)$ plotted versus V for ShB-IR, E293Q, D316N, R365Q, and R368N. R368N and E293Q show saturation, approaching a value of about 6–7 $e_0$. R365Q, ShB-IR, and especially D316N do not show saturation in the voltage range studied. The open circles represent the Q–V curve plotted as $z_{Q/N}(Q_{max} - Q)/Q_{max}$.

$z_{Q/N}$ in the ShB-IR channel, suggesting that, at least for this channel, most or all of the nonlinear charge movement is linked to activation. Therefore, either $z_{Q/N}$ or $z_c$ provides an accurate estimate of z.

The main observation of our study is that, out of eight residues tested, only four, E293 in S2, and R365, R368, and R371 in S4, contribute significantly to the gating charge movement that precedes channel opening. In addition, D316 may make a smaller contribution. Previous results suggested that the S4 residue R368 is involved in gating charge movement: the neutralization mutation R368Q enhances the separation of two components of gating charge movement (Bezanilla et al., 1994) and reduces the proportion of charge transferred by one of the components (Perozo et al., 1994). We have now shown that the mutation R368N reduces z significantly.

Although D316N has effects on the Q–V curve similar to those of R368Q (Figure 2; Perozo et al., 1994), it does not reduce z significantly (p = 0.07) compared with R368N. Because z corresponds to the movement of the voltage sensor, a reduction in z is likely to be more meaningful than alterations in the Q–V curve. The finding that the mutation R371Q reduces z significantly is somewhat surprising. R371Q does not have appreciable effects on either the g–V or Q–V curves (Papazian et al., 1991; Perozo et al., 1994); these results indicate that changes in the slope or the midpoint of steady-state g–V or Q–V curves are not sufficient to implicate a mutated residue in gating charge movement.

Our results indicate that E283 in S2 and K374 (and perhaps R362) in S4 do not move relative to the field during voltage-dependent activation. Although some or

Table 2. Change per Channel Estimated from $Z_s$, $Z_c$, and $Z_{Q/N}$

| Mutant | $z_s$ ($e_0$) Mean $\pm$ SD (n) | Voltage Range for the Estimation of $z_s$ (mV) | Range of $\log(g/g_{max})$ for the Estimation of $z_s$ (mV) | $z_c$ ($e_0$) | $z_{Q/N}$ ($e_0$) |
|---|---|---|---|---|---|
| ShB-IR | >10.9 $\pm$ 1.3 (6) | $-61 \sim -66$ | $-2.5 \sim -3.1$ | 12.6 | 12.9 |
| E283Q | >5.2 $\pm$ 1.1 (4) | $-13 \sim -21$ | $-1.5 \sim -2.3$ | 8.9 | 13.0 |
| E293Q | 7.4 $\pm$ 0.6 (6) | $-54 \sim -62$ | $-2.0 \sim -2.8$ | 7.4 | 6.6 |
| D316N | >4.8 $\pm$ 1.4 (10) | $-41 \sim -49$ | $-2.1 \sim -2.7$ | 10.8 | 11.3 |
| R362Q | >8.7 $\pm$ 2.4 (7) | $-101 \sim -107$ | $-2.6 \sim -3.4$ | — | — |
| R365Q | >5.1 $\pm$ 0.7 (6) | $-81 \sim -89$ | $-2.2 \sim -2.9$ | 8.2 | 8.0 |
| R368N | 5.7 $\pm$ 0.9 (6) | $-66 \sim -78$ | $-1.9 \sim -3.0$ | 5.7 | 6.1 |
| R371Q | 6.3 $\pm$ 0.8 (4) | $-60 \sim -72$ | $-2.0 \sim -3.0$ | 6.3 | 6.9 |
| K374Q+E293Q | 5.9 $\pm$ 0.5 (6) | $-67 \sim -76$ | $-1.7 \sim -2.5$ | 5.9 | 7.4 |
| K374Q+D316N | >7.8 $\pm$ 1.7 (4) | $-92 \sim -98$ | $-1.9 \sim -2.5$ | 9.2 | 11.1 |

$z_s$ was estimated as the mean of S(V) in the voltage range shown in third column. The corrected value of $z_s$, $z_c$, was obtained by adding the missing charge, according to the Q–V curve (see text). $V_s$ corresponds to the middle of the range shown in column 3. The last column shows means of $z_{Q/N}$ in each mutant for comparison with $z_c$.

all of these residues may be out of the transmembrane field, E283 and K374 appear to experience strong, presumably short-range electrostatic interactions with R368 and R371 and with E293, respectively, which are within the field because they contribute to the charge per channel (Papazian et al., 1995; S. Tiwari-Woodruff and D. M. P., unpublished data).

E293Q, R365Q, R368N, and R371Q reduced the charge/channel by as much as 7 $e_0$. If one charged residue traversed the entire transmembrane electric field, it could contribute a maximum of four charges, one per subunit in the tetrameric channel. Therefore, the mutations must have indirect effects on unmutated residues, affecting their movement or the electric field that they traverse, or both. Because of these indirect effects, it is not possible to assign unequivocally a fraction of the charge/channel to a particular residue. Previously, evidence has been presented that charged residues in S2, S3, and S4 experience both strong and weak electrostatic interactions with each other (Papazian et al., 1995); therefore, it is not surprising that neutralizing one position has indirect effects on interacting residues. Considering the large reductions in z, it seems unlikely that the effects of E293Q, R365Q, R368N, and R371Q are entirely indirect, but this possibility cannot be ruled out. The evidence suggests, however, that E293 in S2, and R365, R368, and R371 in S4 constitute a significant part of the voltage sensor in *Shaker* K+ channels. Even if these residues did not move relative to the field, the results indicate that they play a major functional role in shaping the electric field detected by the voltage sensor.

Recently, the environments of residues in the S4 segments of K+ and Na+ channels have been probed with sulfhydryl reagents after cysteine substitution mutagenesis (Yang and Horn, 1995; Larsson et al., 1996; Yang et al., 1996). In the *Shaker* channel, voltage-dependent reactivity of cysteine residues substituted for R365 and R368 in the S4 segment has been reported, providing evidence that the environment of the S4 segment changes upon activation (Mannuzzu et al., 1996; Larsson et al., 1996). In the muscle sodium channel, the reactivity of the second and third positively charged residues in the S4 segment of the fourth domain switches from one side of the membrane to the other upon depolarization, providing evidence that these positions traverse the field during activation (Yang et al., 1996). However, these experiments do not measure the contribution of these residues to the gating charge.

The results reported here provide direct evidence that one negatively charged residue and three positively charged residues constitute a major portion of the nonlinear charge movement responsible for the gating of *Shaker* K+ channels. It is significant that of the S4 residues that we have tested, R365, R368, and R371, which are located in the center of the segment, contribute to the gating charge. This could be explained by assuming that the other charges are exposed to solvent, and thus are outside of the electric field, or that the movement of the segment does not occur as a unit, or both. These results suggest that the electric field is focused in the central part of the S4 segment, in agreement with the proposal of Yang et al. (1996), indicating that only small conformational changes might be needed to transfer significant amounts of charge across the transmembrane field, leading to channel opening.

## Experimental Procedures

### Site-Directed Mutagenesis
Mutations were generated in a Bluescript subclone of the *Shaker* B cDNA clone (Schwarz et al., 1988) by oligonucleotide-directed mutagenesis on a single-stranded template (Kunkel et al., 1987) or by PCR (Horton et al., 1989). Mutations were verified by sequencing. cRNA was prepared and injected into Xenopus oocytes as previously described (Timpe et al., 1988).

### Electrophysiology
#### Recording Solutions
The following solutions were used in electrophysiological experiments. Internal 120 K+ solution: 120 mM K–methanesulphonic acid (MES), 10 mM HEPES, and 1 mM EGTA–N-methylglucamine (NMG). External 120 K+ solution: 120 mM K–MES, 10 mM HEPES, and 1.8 mM CaCl$_2$. Internal 0 K+ solution: 110 mM NMG–MES, 10 mM HEPES, and 10 mM EGTA–NMG. External 0 K+ solution: 110 mM NMG–MES, 10 mM HEPES, and 2 mM CaCl$_2$. After recording 150–200 ionic current traces for fluctuation analysis, ionic currents were blocked in inside-out patches by bath application of 110 mM TEA–MES or 110 mM NMG–MES, 10 mM HEPES, and 10 mM EGTA–NMG. The following solutions were used for gating current measurements at the reversal potential in cell-attached or inside-out patch mode. Internal 1 K+ solution: 1 mM K–MES, 110 mM NMG–MES, 10 mM HEPES, and 10 mM EGTA–NMG. External 1 K+ solution: 1 mM K–MES, 110 mM NMG–MES, 10 mM HEPES, and 2 mM CaCl$_2$. The osmolarity of all solutions was adjusted to 240–250 mOsm, and the pH was adjusted to 7.2.

#### Procedure to Estimate $z_{Q/N}$ with Gating and Ionic Currents
The total nonlinear charge movement per channel was calculated by dividing the time integral of the gating current (Q) by the number of channels (N). N was obtained from nonstationary fluctuation analysis of an ensemble of 150 macroscopic ionic currents recorded under identical conditions (Sigworth, 1980). The ensemble mean current (I) and variance ($\sigma^2$) as a function of time were fitted to the equation $\sigma^2 = iI - I^2/N$, where i is the open channel unitary current. To minimize the effects of drift on the measurement of the ensemble variance, sample variances were calculated for overlapping pairs of records, and the results were then averaged over all pairs (Sigg et al., 1994). Experiments in which the amplitude of the ionic current varied by more than 10% were discarded. In most of the experiments, the patch pipette contained 0 K+ NMG–MES solution, while the bath contained 120 K–MES. After a total of about 150 ensemble traces were recorded in inside-out patches, the bath was replaced with NMG–MES or TEA–MES to eliminate ionic current. The gating current was then measured with a p/4 protocol with the subtraction holding potential being more depolarized than the test pulse. In some of the experiments, perforated oocytes were allowed to equilibrate in a 1 mM K+ solution for 20–30 min and a 1 mM K+ solution was added to the pipette as well. In this way, gating currents could be recorded without excising by pulsing to the reversal potential (typically −9 to 1 mV). Because ionic tail currents were generated under these conditions, fluctuation analysis could be applied to both the activation and deactivation currents.

The effective total valence $z_{Q/N}$ was computed from $Q = z_{Q/N}\delta e_0 N$, where the electronic charge $e_0 = 1.6 \times 10^{-19}$ C, and $\delta$ is a factor representing the weighted sum of fractional displacements traversed by the participating physical charges. Obtaining an estimate for $\delta$ is not possible using our methods, so we arbitrarily set it equal to unity. The open probability at maximal activation ($P_o$) was estimated by dividing the ionic current by the product of i and N.

Experimental conditions were similar for all experiments. All patches were in the inside-out configuration using borosilicate glass pipettes with approximately 0.5–1 M$\Omega$ resistance. Filtering was done with an 8 pole Bessel filter at 10 kHz while the acquisition rate was 50 kHz. The temperature was 21°C–23°C.

#### Limiting Slope Procedure
With this procedure, $z_s$ was estimated by measuring a quantity proportional to the relative open probability $P_o$ at a range of very negative potentials where $P_o$ approaches zero (Almers, 1978). In these

limiting conditions, ln($P_o$) is proportional to $z_s \delta e_0 V/kT$, where V is the membrane potential and k is Boltzmann's constant. Again, we set $\delta = 1$. To record the ionic currents, we used a ramp protocol in the cell-attached patch mode starting from −140 and ending at +10 mV in symmetrical 120 mM/120 mM $K^+$ solutions with a duration ranging from 450 ms to 1 s. We could not safely increase the duration due to complications brought on by slow inactivation of the ionic current. The leakage current ($I_{leak}$) at very negative potentials was fit to a straight line and was subtracted from the record to obtain the ionic current ($I_{ionic}$). The conductance (g) was calculated using the equation, $g = I_{ionic}/(V − V_{rev})$. The value of g is equal to $N\gamma P_o$, where $\gamma$ is the single-channel conductance and N is the number of channels in the patch. $\gamma$ was constant, as revealed by the instantaneous I–V relation. It was frequently possible to measure g at voltages where $P_o/P_{max}$ reached values less than $10^{-3}$. A quantity S was computed as the first derivative of the natural logarithm of $N\gamma P_o$ with respect to V and multiplied by $kT/e_0$. The derivative was computed by subtracting consecutive points and making running averages of neighboring points to maintain resolution of about 1–4 mV. The values of S were plotted with respect to V. In the limit, when $V \sim -\infty$, S should converge to the actual value of z. A major concern was whether the ramp speed (dV/dt) was too fast to measure properly equilibrium values of the open probability. The value of S(V) in the region of low open probability did not change significantly after reducing dV/dt by 50%. In some experiments, we were able to extend the measurements to even lower values of $P_o$ by measuring an ensemble of currents elicited by the same voltage ramp restricted to the region of negative potentials (−140 to −60 mV). From the ensemble of currents, we computed the ensemble variance, which was divided by the square of the open channel current to estimate the $P_o$. This is because $\sigma^2 = Ni^2 P_o(1 − P_o)$, which becomes $Ni^2 P_o$ when $P_o$ is very small. All experiments were performed at 19°C–23°C.

### References

Almers, W. (1978). Gating currents and charge movements in excitable membranes. Rev. Physiol. Biochem. Pharmacol. 82, 96–190.

Armstrong, C.M., and Bezanilla, F. (1973). Currents related to movement of the gating particles of the sodium channels. Nature 242, 459–461.

Bezanilla, F., Perozo, E., Papazian, D.M., and Stefani, E. (1991). Molecular basis of gating charge immobilization in Shaker potassium channels. Science 254, 679–683.

Bezanilla, F., Perozo, E., and Stefani, E. (1994). Gating of Shaker $K^+$ channels. II. The components of gating currents and a model of channel activation. Biophys. J. 66, 1011–1021.

Catterall, W.A. (1986). Molecular properties of voltage-sensitive sodium channels. Annu. Rev. Biochem. 55, 953–985.

Chandy, G., and Gutman, G.A. (1995). Voltage-gated potassium channel genes. In Handbook of Receptors and Channels: Ligand- and Voltage-Gated Ion Channels, R.A. North, ed. (Boca Raton, Florida: CRC Press), pp 1–70.

Guy, H.R., and Seetharamulu, P. (1986). Molecular model of the action potential sodium channel. Proc. Natl. Acad. Sci. USA 83, 508–512.

Hamill, O.P., Marty, A., Neher, E., Sakmann, B., and Sigworth, F.J. (1981). Improved patch-clamp techniques for high-resolution current recording from cells and cell-free membrane patches. Pflügers Arch. 391, 85–100.

Hodgkin, A.L., and Huxley, A.F. (1952). A quantitative description of membrane current and its application to conduction and excitation in nerve. J. Physiol. 117, 500.

Horton, R.M., Hunt, H.D., Ho, S.N., Pullen, J.K., and Pease, L.R. (1989). Engineering hybrid genes without the use of restriction enzymes: gene splicing by overlap extension. Gene 77, 61–68.

Hoshi, T., Zagotta, W.N., and Aldrich, R.W. (1990). Biophysical and molecular mechanisms of Shaker potassium channel inactivation. Science 250, 533–538.

Kunkel, T.A., Roberts, J.D., and Zakour, R.A. (1987). Rapid and efficient site-specific mutagenesis without phenotypic selection. Meth. Enzymol. 154, 367–382.

Larsson, H.P., Baker, O.S., Dhillon, D.S., and Isacoff, E.Y. (1996). Transmembrane movement of the Shaker $K^+$ channel S4. Neuron 16, 387–397.

Li, M., Unwin, N., Stauffer, K.A., Jan, Y.N., and Jan, L.Y. (1994). Images of purified Shaker potassium channels. Curr. Biol. 4, 110–115.

Liman, E.R., Hess, P., Weaver, F., and Koren, G. (1991). Voltage-sensing residues in the S4 region of a mammalian $K^+$ channel. Nature 353, 752–756.

Logothetis, D.E., Movahedi, S., Satler, C., Lindpaintner, K., and Nadal-Ginard, B. (1992). Incremental reductions of positive charge within the S4 region of a voltage-gated $K^+$ channel result in corresponding decreases in gating charge. Neuron 8, 531–540.

MacKinnon, R. (1991). Determination of the subunit stochiometry of a voltage-activated potassium channel. Nature 350, 232–235.

Mannuzzu, L.M., Moronne, M.M., and Isacoff, E.Y. (1996) Direct physical measure of conformational rearrangement underlying potassium channel gating. Science 271, 213–216.

Noda, M., Shimizu, S., Tanabe, T., Takai, T., Kayano, T., Ikeda, T., Takahashi, H., Nakayama, H., Kanaoka, Y., Minamino, N., et al. (1984). Primary structure of Electrophorus electricus sodium channel deduced from cDNA sequence. Nature 312, 121–127.

Papazian, D.M., Timpe, L.C., Jan, Y.N., and Jan, L.Y. (1991). Alteration of voltage-dependence of Shaker potassium channel by mutations in the S4 sequence. Nature 349, 305–310.

Papazian, D.M., Shao, X.M., Seoh, S.-A., Mock, A.F., Huang, Y., and Wainstock, H. (1995). Electrostatic interactions of S4 voltage sensor in Shaker $K^+$ channel. Neuron 14, 1293–1301.

Perozo, E., MacKinnon, R., Bezanilla, F., and Stefani, E. (1993). Gating currents from a nonconducting mutant reveal open-closed conformations in Shaker $K^+$ channels. Neuron 11, 353–358.

Perozo, E., Santacruz-Toloza, L., Stefani, E., Bezanilla, F., and Papazian, D.M. (1994). S4 mutations alter gating currents of Shaker K channels. Biophys. J. 66, 345–354.

Planells-Cases, R., Ferrer-Montiel, A.V., Patten, C.D., and Montal, M. (1995). Mutation of conserved negatively charged residues in the S2 and S3 transmembrane segments of a mammalian $K^+$ channel selectively modulates channel gating. Proc. Natl. Acad. Sci. USA, 92, 9422–9426.

Schoppa, N.E., McCormack, K., Tanouye, M.A., and Sigworth, F.J. (1992). The size of gating charge in wild-type and mutant Shaker potassium channels. Science 255, 1712–1715.

Schwarz, T.L., Tempel, B.L., Papazian, D.M., Jan, Y.N., and Jan, L.Y. (1988). Multiple potassium-channel components are produced by alternative splicing at the Shaker locus in Drosophila. Nature 331, 137–142.

Sigg, D., Stefani, E., and Bezanilla, F. (1994). Gating current noise produced by elementary transitions in Shaker potassium channels. Science 264, 578–582.

Sigworth, F.J. (1980). The variance of sodium current fluctuations at the node of Ranvier. J. Physiol. 307, 97–129.

Stefani, E., Toro, L., Perozo, E., and Bezanilla, F. (1994). Gating of

Shaker K$^+$ channels. I. Ionic and gating currents. Biophys. J. *66*, 996–1010.

Stuhmer, W., Conti, F., Suzuki, H., Wang, X.D., Noda, M., Yahagi, M., Kubo, H., and Numa, S. (1989). Structural parts involved in activation and inactivation of the sodium channel. Nature *339*, 597–603.

Timpe, L.C., Schwarz, T.L., Tempel, B.L., Papazian, D.M., Jan, Y.N., and Jan, L.Y. (1988). Expression of functional potassium channels from Shaker cDNA in *Xenopus* oocytes. Nature *331*, 143–145.

Yang, N., and Horn, R. (1995). Evidence for voltage-dependent S4 movement in sodium channels. Neuron *15*, 213–218.

Yang, N., George, A.L., and Horn, R. (1996). Molecular basis of charge movement in voltage-gated sodium channels. Neuron *16*, 113–122.